

Preparation of polyacrylamide grafted collagen extracted from leather wastes and their application in kaolin flocculation

Chongyi Li, Feng Xue, Enyong Ding

Department of Polymer Science, College of Material Science and Engineering, South China University of Technology, Guangzhou 510641, People's Republic of China

Correspondence to: E. Ding (E-mail: eyding@scut.edu.cn)

ABSTRACT: This is probably the first report on the synthesis of a series of novel collagen-based flocculants (CP11, CP12, and CP13) by grafting polyacrylamide (PAM) chains onto the collagen backbone, which was directly extracted from leather shavings via alkali hydrolysis. The results from FTIR, XRD, ^1H NMR, and TGA well supported that PAM chains had been successfully grafted onto collagen backbone. In addition, the micrographs of SEM revealed that the PAM grafted collagen possessed much more porous and looser surface structures in comparison with virgin collagen. Zeta potential measurement showed that the introduction of branched PAM chains helped to improve the positively charge density. Furthermore, CP12 performed the best in the kaolin flocculation with the highest flocculation rate about $24\% \cdot \text{min}^{-1}$ and could induce the generation of much larger and denser floccs for the fast settling of kaolin particles. The corresponding flocculation mechanism was also presented by analyzing the collected floccs. © 2014 Wiley Periodicals, Inc. *J. Appl. Polym. Sci.* **2015**, *132*, 41556.

KEYWORDS: biopolymers and renewable polymers; grafting; properties and characterization

Received 4 June 2014; accepted 24 September 2014

DOI: 10.1002/app.41556

INTRODUCTION

As is well-known that water is an origin of life, a material basis for all the human existence and social economic growth, and a principal guarantee for the sustainable development. Efficient treatments on the various effluents, which are discharged by industrial production inevitably, have drawn great attention all the time, due to the growing environmental concerns.^{1–4} Especially in the last few years, the increasing enthusiasm and interest on water conservation have greatly accelerated the extensive researches on wastewater treatment, and many physicochemical methods including flocculation,^{5,6} photocatalytic degradation,^{7–9} activated carbon absorption,^{10,11} etc, have been employed for effluent purification. However, among them, flocculation is still considered as one of the most significant measures used for pre-treatment or primary treatment of effluents, owing to its high efficiency and facile operation.

Although inorganic metal-based flocculants and synthetic polymer-based flocculants are always popular in wastewater clarification, we must also attach importance to their unwelcome disadvantages that continually accumulated metal ions and harmful monomers produced by partial degradation of polymeric flocculants will generate potentially adverse impacts on the ecological system. Thus, a novel environmental friendly, cost-effective and more efficient flocculant is desired strongly.

At present, much more attentions have been shifted to the application of natural polymers for flocculant development, such as cellulose,¹² chitosan,^{13–15} starch,^{16–18} sodium alginate,¹⁹ and guar gum.^{20,21} In comparison with traditional flocculants, these natural polymer-based flocculants can become attractive alternatives because of their biodegradability, easy availability, and low cost. More significantly, these modified natural macromolecule products have been well proved to be excellent flocculants for the various wastewaters treatment.^{22–27}

Actually, as the suspension stability of kaolin-containing effluents from mining industry, it is very difficult for kaolin to be fast settling and removed absolutely, which is caused by strong electrostatic repulsion between particles. Therefore, it may be a novel subject to use amphoteric collagen to fabricate an exclusive and efficient flocculant for kaolin flocculation. However, researches can rarely be found both at home and abroad on using collagen sourced from leather solid wastes in flocculant field, say nothing of systematic analysis and study. As one of the most abundant natural biomass, collagen has attracted broad interest and been particularly exploited to produce a series of novel functional materials.^{28–31} Collagen is a special amphoteric protein due to the presence of plentiful $-\text{NH}_2$ groups and $-\text{COOH}$ groups on its molecular chains, which can contribute to the removal of many impurities with charges

theoretically, on the basis of widely accepted perspective of charge attraction. Consequently, collagen is capable for processing complicated wastewater as an eligible candidate. Nevertheless, significant importance should also be attached to the following two principal known disadvantages: firstly, the isoelectric point of collagen is located at pH below 7 usually, which indicate that relatively less quantity of $-\text{NH}_2$ groups is adverse for sedimentation of kaolin particles; secondly, a too short shelf life derived from its good biodegradability also needs to be appropriately improved. Taking into consideration that adsorption bridging and net-sweeping effects are also the crucial influence factors on flocculation, graft polymerization can be used as an effective means to overcome the above shortcomings.^{22,32} As everyone knows that polyacrylamide (PAM) has exhibited high efficiency in wastewater purification, and grafting PAM chains onto collagen backbone can not only enhance the density of $-\text{NH}_2$ groups, but also can benefit for the improvement of bridging and net-sweeping effect, which are induced by the long PAM branched chains. However, no researches have been done on using PAM grafted collagen as a tailor-made flocculant for promoting kaolin flocculation.

Up to now, an enormous amount of chromed leather wastes produced by tanning industry have been regarded as a troublesome problem for many years. These leather wastes are composed of fibrous collagen stabilized by trivalent chromium in a three dimensional structure. Nevertheless, the current disposal ways for the leather wastes including incineration and landfill, may bring about unnecessary resource waste and potential contamination risk, because trivalent chromium (Cr^{3+}) can oxidize into virulent hexavalent chromium (Cr^{6+}) under certain temperature and pH condition.^{33,34} Facing such severer challenge, unremitting efforts have been made for the high value-added utilization of these leather wastes,^{35–37} while it may after all be accepted as a significant pattern for resource recycling that collagen is extracted from leather wastes and then used for preparing a novel effective flocculant.

In view of all the aspects as mentioned above, this article aims to develop a novel efficient and eco-friendly flocculant for the rapid settlement of kaolin suspensions. The acrylamide was selected as modified monomer to graft onto collagen backbone, which was directly extracted from leather shavings via alkali hydrolysis, by using ceric ammonium nitrate as the initiator, followed that a series of collagen-g-PAM products with different weight feeding ratios were successfully synthesized. The resulting products were comprehensively characterized by Fourier transform infrared (FTIR), X-ray diffraction (XRD), scanning electron microscope (SEM), zeta potential measurement, ^1H nuclear magnetic resonance spectroscopy (^1H NMR), and thermogravimetric analysis (TGA). In addition, their properties for kaolin flocculation were investigated systematically by using the jar test method, and the corresponding flocculation mechanism was also proposed.

EXPERIMENTAL

Materials

Chromed leather shavings from cattle skin were donated by a tannery in the province of Zhejiang, China; kaolin (AR grade, 3000 mesh), calcium oxide (CP grade), acrylamide (AR grade),

and ceric ammonium nitrate (AR grade) were supplied by Aladdin Industrial Corporation, China. Deionized water was used throughout the study, and all the chemicals were used as received without further purification.

Extraction of Collagen

Collagen was extracted from chromed leather shavings via alkaline hydrolysis. First of all, a desired amount of leather shavings was immersed into water at an appropriate ratio of material to water for 1 h. Then, calcium oxide was added to the above dispersion at a mass concentration of 8% on leather shavings. After reacting for 6 h at 85°C , this mixture was filtered under vacuum to separate the chrome cake and collect collagen solution, followed that this collagen solution was adjusted to be neutral with dilute HCl solution. Finally, the obtained collagen solution was concentrated by rotary evaporator, precipitated, and washed repeatedly by absolute ethyl alcohol, and next dried to powders in the oven. Based on the results from GPC, the molecular weight of collagen powders acquired was estimated. ($M_n = 4.1 \times 10^3$ Da and $M_w = 7.43 \times 10^3$ Da).

Synthesis of Collagen-g-PAM Flocculants

A given amount of collagen powders were dissolved in the deionized water with a constant stirring under N_2 atmosphere until this solution became clear and yellowish; followed that a fixed amount of ceric ammonium nitrate as initiator was added into the above solution; and then the acrylamide monomer aqueous solution was added dropwise within 30 min after 10 min of pretreatment by the initiators to trigger abundant active grafting points on the collagen backbone. The reaction system was protected by N_2 atmosphere in the whole process. After reacting at 50°C for 5 h, the primary product was precipitated in the excess absolute ethyl alcohol and then collected by centrifugalization. Furthermore, the obtained products were extracted in Soxhlet apparatus using acetone as solvent for 48 h to remove impurities. Finally, the purified products were vacuum-dried at 60°C for 48 h. By the way, three grafted samples with different weight feeding proportion between collagen and acrylamide (1 : 1, 1 : 2, and 1 : 3) were synthesized, which were named CP11, CP12, and CP13, respectively. The possible reaction mechanism was also proposed as follows: based on free radical theory, grafting polymerization of acrylamide onto collagen backbone initiated by oxidation-reduction initiator systems was carried out. Typically, the presence of abundant highly reactive groups with strong reducibility like $-\text{NH}_2$ and $-\text{OH}$ made collagen readily oxidized to some extent. Thus, as a strong oxidant, Ce^{4+} could be reduced to Ce^{3+} by gaining electrons from these groups; meanwhile, collagen chains were transformed into macromolecule radicals immediately, which would attack $\text{C}=\text{C}$ bonds in the acrylamide for triggering violent chain propagation reaction until chain termination reaction took place. Inevitably, polymerization of acrylamide also spontaneously proceeded simultaneously, which would compete with grafting reaction fiercely. Consequently, the obtained products must be purified carefully.

Characterization

Infrared Analysis. The collagen and grafted collagen were evaluated by using Fourier transformed infrared spectrometer

(Nicolet, MAGNA-IR760) with KBr pellet method at wave numbers from 650 to 3800 cm^{-1} .

X-ray Diffraction. The aggregation structures of collagen and grafted collagen were characterized by the XRD performed on a MSALXD2 with Cu K α radiation (40 kV, 20 mA, $\lambda = 1.54051$ Å) at a scanning rate of 5°/min for 2θ ranging from 5° to 75°.

Filed Emission Scanning Electron Microscopy

The morphology of collagen and grafted collagen were observed by using a field emission scanning electron microscopy (Nova-NanoSEM 430) operated at an accelerating voltage of 10 kV.

Thermogravimetric Analysis

The thermal stabilities of collagen and grafted collagen were studied by NETZSCH TG209F1, and all the specimens were scanning from 25 to 800°C in nitrogen atmosphere at a heating rate of 20°C/min.

^1H Nuclear Magnetic Resonance

^1H NMR spectra of collagen and grafted collagen were obtained on a Bruker AVANCE Model DRX-500 spectrometer, operating at 500 MHz and using D_2O as the solvent.

Zeta Potential Analysis

Zeta potential of collagen and grafted collagen were measured by a Malvern Model Zetasizer (NanoZS 90) manufactured in U.K.

Flocculation Experiment

Experiments on flocculating the kaolin suspensions were performed by using the conventional jar test method and their pH were regulated to the desired values with dilute HCl aqueous solutions. The flocculation efficiencies of virgin collagen and grafted collagens with varied synthesized grades were evaluated synthetically. Specially, a desired amount of flocculants were added into the 3 g/L of kaolin suspension in the form of solution first; thereafter, this mixture was stirred strongly at a speed of 300 rpm for 2 min at the beginning, followed by a slow stirring at 50 rpm for next 3 min, and then the suspension was allowed to settle for 5 min. During the settling period, it could be observed distinctly that the breaker deposited a large amount of kaolin particles at its bottom, and the supernatant suspension became clear gradually.

After sedimentation for 5 min, a 4 mL of supernatant suspension was withdrawn, and the flocculation efficiency was determined by UV-visible spectrophotometry (UNICAM UV-500, Thermo Electron Co.). A calibration curve for kaolin suspensions was measured in advance. The transmittances of the supernatant suspensions were detected at a wavelength of 641 nm, which was used to reflect the flocculation abilities of various synthesized flocculants. In addition, the formed flocs were also collected for further morphological observation by using optical microscopy and FTIR analysis.

RESULTS AND DISCUSSION

Chemical Structure

The FTIR spectra of acrylamide, extracted collagen as well as PAM grafted collagen with various synthetic grades were illustrated in Figure 1. As was seen clearly that the spectrum of acrylamide showed the characteristic absorption peaks at

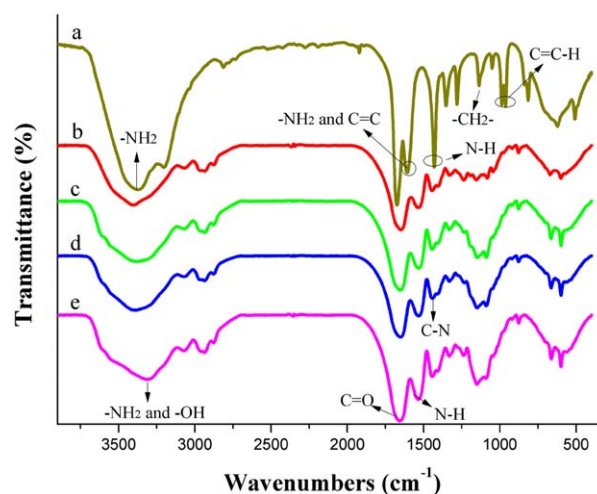


Figure 1. FTIR spectra of the various samples: (a) acrylamide; (b) virgin collagen extracted from leather shavings; (c) CP11; (d) CP12; (e) CP13. [Color figure can be viewed in the online issue, which is available at wileyonlinelibrary.com.]

3400 cm^{-1} ($-\text{NH}_2$ stretching), 3203 cm^{-1} ($=\text{C}-\text{H}$ stretching), 1672 cm^{-1} (amide I, $\text{C}=\text{O}$ stretching), 1620 cm^{-1} (amide II, $-\text{NH}_2$ bending), 1420 cm^{-1} ($\text{N}-\text{H}$ stretching) and 983 cm^{-1} ($=\text{C}-\text{H}$ wagging vibration). Obviously, the characteristic peak of $\text{C}=\text{C}$ stretching, which should also be present at 1620 cm^{-1} approximately, overlapped with that of amide II. While in the spectrum of collagen pattern, a broad characteristic absorption peak around 3400 cm^{-1} was ascribed to the strong $\text{O}-\text{H}$ and $\text{N}-\text{H}$ stretching vibration, in addition, two indistinctive peaks located at 2975 and 2946 cm^{-1} as well as the other weak peak around 2869 cm^{-1} could be attributed to asymmetric and symmetric stretching vibration of $-\text{CH}_3$ and the symmetric stretching of $-\text{CH}_2-$, respectively. An obvious but small peak located at 3072 cm^{-1} was the powerful evidence indicating the presence of benzene ring. Besides, the band at 1665 cm^{-1} arose from $\text{C}=\text{O}$ stretching vibration while the other adjacent intensive peak around 1545 cm^{-1} was for $\text{N}-\text{H}$ bending vibration, which was due to the existence of polypeptide chain in collagen. Furthermore, there were three bands at 1454, 1165, and 1076 cm^{-1} , which were assigned to $\text{C}-\text{N}$ stretching in $\text{C}-\text{NH}_2$, $-\text{CH}_2-$ wagging vibration and $\text{C}-\text{N}$ bending, respectively. By contrast, in the case of PAM grafted collagen, although there were no additional peaks present, the intensities of $\text{C}-\text{N}$ stretching (1454 cm^{-1}), $-\text{CH}_2-$ wagging vibration (1165 cm^{-1}) and $\text{C}-\text{N}$ bending (1076 cm^{-1}) were enhanced significantly with the addition of acrylamide monomer increasing gradually, which powerfully proved that PAM chains had been grafted onto collagen backbone successfully.

TGA Analysis

The thermal degradation behaviors of collagen as well as PAM grafted collagen were investigated by thermogravimetry (TGA), and the occurrence of efficient graft modification was also well proved based on the TGA results. As was shown in Figure 2 that the thermal degradation of virgin collagen mainly involved two stages: for the first step in the temperature range from 25 to 184°C, the absorbed and bound water was lost with the

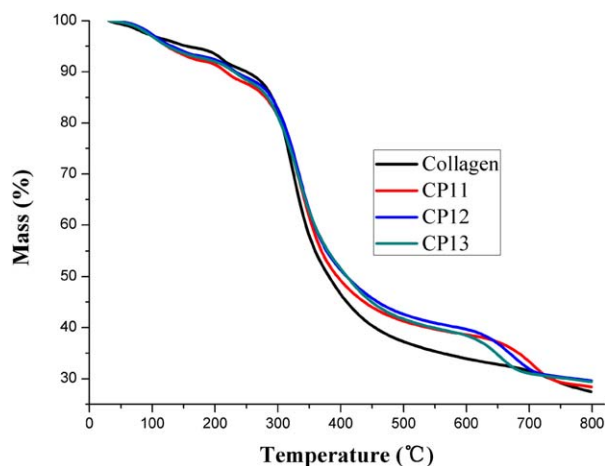


Figure 2. TGA curves for virgin collagen and various PAM grafted collagens. [Color figure can be viewed in the online issue, which is available at wileyonlinelibrary.com.]

weight loss about 8 wt %, while the second stage started at 240°C and continued up to 800°C with the maximal degradation temperature at 350°C, which could be associated with the ultimate breakage of collagen backbone. Obviously, the pyrolysis properties of PAM grafted collagen had been varied dramatically in comparison with the virgin collagen. In the case of the modified products, the additional third degradation stages were attributed to the destruction of the PAM branched chains, whose degradation temperatures were far higher than that of collagen chains. This increase could be interpreted that the presence of other heteroatoms such as O, N in the main chains of collagen made them much easier than PAM grafted chains to be broken at a lower temperature. The appearances of these additional stages were the strongest proofs for supporting the successful graft polymerization. In addition, their maximal decomposition temperatures decreased in turn as the weight feeding ratio of acrylamide monomers increased, which indicated that the addition of excessive acrylamide might be inclined to form shorter branched chains easily, because for PAM branched chains with well-defined composition and structure, the higher the degradation temperature was, the higher the molecular weight was, and correspondingly, the longer the molecular chain was to a certain extent, and vice versa. The reason for this result was based on the fact that with the constant reaction time and the amount of initiator, too many acrylamide monomer added necessarily caused a sharp increase in the possibility of self-polymerization, which was bound to make relatively less amount of acrylamide monomers involved in grafting reaction, because of depletion in the available acrylamide concentration as the self-polymerization occurred, which was also responsible for the decrease of size of PAM grafted chains. Apparently, there was a healthy weight feeding ratio between collagen and acrylamide for preparing modified collagen, which had PAM branched chains with appropriate length. Moreover, the thermal stabilities of collagen chains for modified products were also improved markedly, and there were much higher moisture content in the modified collagen, because of introduction of abundant $-\text{NH}_2$ groups.

XRD Analysis

The XRD patterns of virgin collagen as well as the modified products were presented in Figure 3 to investigate their aggregation structures. As exhibited in Figure 3 that the virgin collagen showed strong crystallization characteristics. However, it was widely known that leather shavings were nearly amorphous,³⁸ which indicated that the collagen chains were deprived of cross-linked constraints from Cr^{3+} and could be rearranged to constitute ordered crystalline regions, due to the alkaline hydrolysis of chromed leather shavings. The collagen contains high content of glycine, which is the indispensable requirement for the formation of natural triple-helical structure, so that glycine is the most critical factor for shaping the aggregation structure of collagen. Evidently, the peaks at 20.7°, 29.1°, and 31.2° could be attributed to α -crystals of glycine, whose corresponding crystalline d-spacing were 0.43, 0.31, and 0.29 nm, respectively; while the other two peaks at 23.4° and 33.4° were ascribed to γ -crystals of glycine, corresponding with crystalline d-spacing about 0.38 and 0.27 nm. In addition, the β -crystals of glutamic acid with crystalline d-spacing about 0.77 nm were confirmed by the presence of characteristic peak around 11.5°. By contrast, although the modified products showed the similar peaks as virgin collagen, some corresponding peaks had shifted even disappeared completely because grafting PAM branched chains onto collagen could strongly inhibit the crystallization of glycine and glutamic acid. Compared with virgin collagen, the intensities of all the crystalline peaks of modified collagen were severely weakened, which implied that organized and tightly arranged collagen chains were significantly disturbed by the inserted PAM moiety. Typically, for the modified collagen, the peak representing β -crystals of glutamic acid, whose intensities weakened continuously as the weight feeding ratio of acrylamide increased, had shifted from 11.5° to 14.7°, which also indicated that its corresponding interplanar d-spacing had clearly reduced from 0.77 to 0.61 nm; similarly, the same tendency could be observed for the characteristic peak of γ -crystals of glycine at 25.6°, accompanying with interplanar d-spacing decreasing from 0.38 to 0.35 nm slightly. In particular, the two sharp peaks,

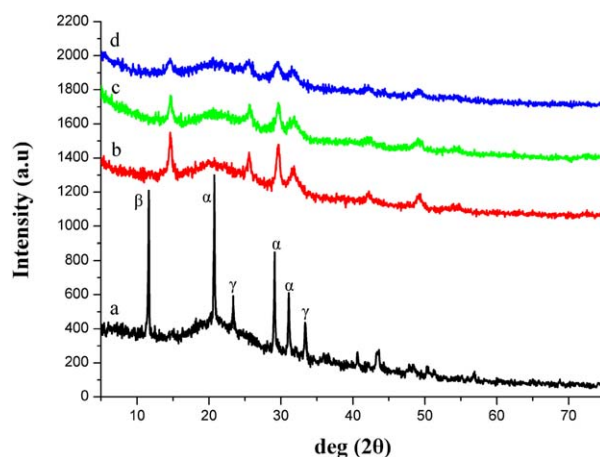
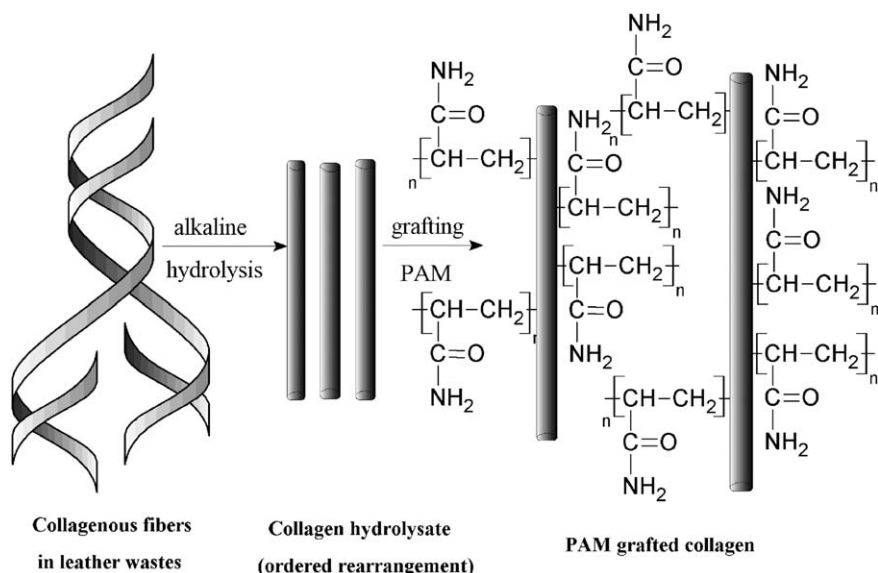


Figure 3. X-ray diffractograms of (a) virgin collagen; (b) CP11; (c) CP12; (d) CP13. [Color figure can be viewed in the online issue, which is available at wileyonlinelibrary.com.]



Scheme 1. Schematic representation for illustrating the variations from the aggregation structures of the PAM grafted collagens.

respectively symbolizing α -crystals (20.7°) and γ -crystals (33.4°) of glycine, had vanished absolutely. There was no doubt that the difference from internal structure would cause the changes in flocculation ability inevitably. The high crystalline structure of virgin collagen derived from regular arrangement of linear polypeptide chains in dependence on the strong hydrogen-bonding interaction, which was responsible for their own limited flocculation abilities due to absence of enough $-\text{NH}_2$ groups able to be protonated and branched chains with appropriate length. This phenomenon was very similar to that of cellulose,³⁹ chitosan,^{40,41} and starch,⁴² which also performed much poorly in flocculation before modification. Obviously, the significance of grafted PAM branched chains lied in decreasing collagen crystallinity, which could benefit for significant improvement of flocculation ability, because PAM branched chains not only provided abundant $-\text{NH}_2$ groups, which could

be protonated for enhancing electrostatic attraction between flocculants and kaolin particles, but also greatly improved bridging and net-sweeping effect, which contributed to netting the suspended kaolin particles much more, better and faster. The corresponding schematic representation for explaining the variation from aggregation structures were shown in Scheme 1.

NMR Analysis

The chemical structures of collagen and the corresponding grafted products were also characterized by ^1H NMR spectroscopy in Figures 4 and 5. It was quite evident that the peaks for all the samples were too indistinguishable and intricate to provide the explicit peak identification, because the ingredients of collagen, which was obtained from alkaline hydrolysis of chromed leather shavings, were very complicated and fairly difficult for the specific assignments essentially. However, by

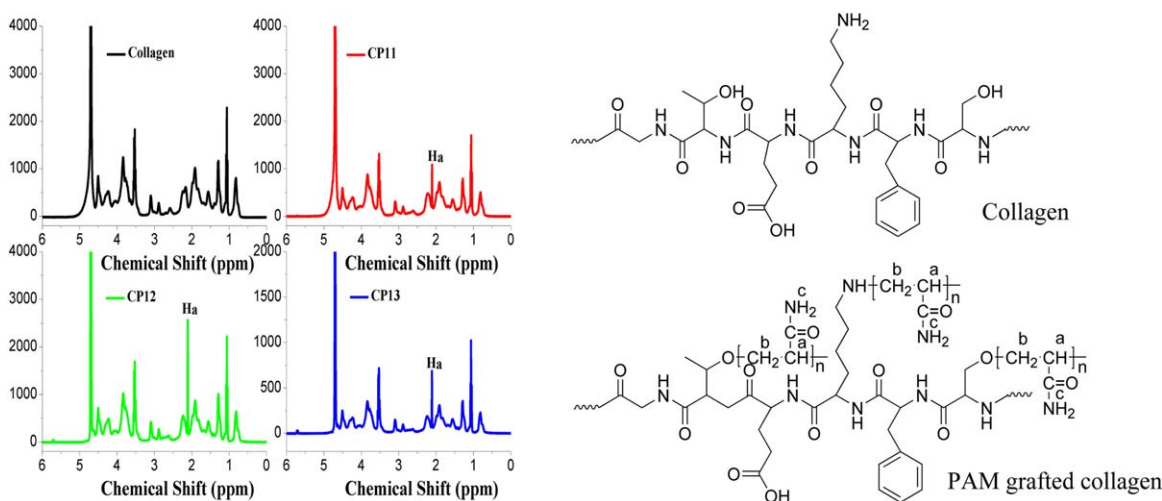


Figure 4. ^1H NMR spectra of virgin collagen and various PAM grafted collagens. [Color figure can be viewed in the online issue, which is available at wileyonlinelibrary.com.]

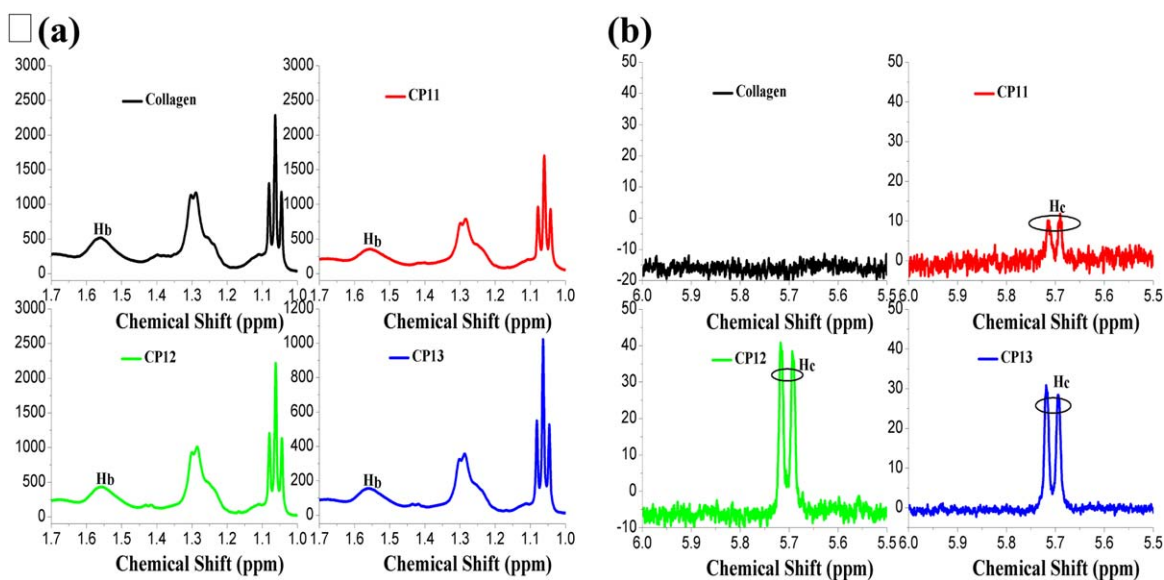


Figure 5. ^1H NMR spectra of virgin collagen and various PAM grafted collagens (as enlarged scale). [Color figure can be viewed in the online issue, which is available at wileyonlinelibrary.com.]

comparing virgin collagen with the PAM grafted collagen, there was a crucially sharp peak ($\delta = 2.1$ ppm) present in the modified collagens, which was assigned to the H_a protons in acrylamide; in addition, the two emerging adjacent peaks not available before, which were located between 5.6 and 5.8 ppm, belonged to H_c from $-\text{NH}_2\text{C}=\text{O}$ groups in acrylamide. Apparently, the presence of these additional peaks clearly supported that grafting PAM chains onto collagen backbone had been carried out successfully. Moreover, the relative intensities of peak at $\delta = 1.56$ ppm corresponded to the H_b protons totally showed little change, indicating that plentiful $-\text{CH}_2-$ groups existed in the collagen chains originally. The grafting ratio (G) of modified collagens could be determined by precisely calculating the relative area of characteristic peaks, which were 67.3, 82.1, and 70.4% for CP11, CP12, and CP13, respectively. Typically, the evaluation on grafting ratio was established depending on the normalized characteristic peaks located at $\delta = 2.1$ and 1.06 ppm, whose relative areas were used to represent the content of the grafted products and virgin collagen, respectively. According to the following defined equation:

$$G = \frac{I_g - I_c}{I_g}$$

where I_g and I_c were the relative area of grafted products and virgin collagen at the same peak position, respectively.

Zeta Potential Measurement

As everyone know that charge characteristics of flocculants played an important role in the flocculation process. Thus, variations of zeta potential of virgin collagen and grafted collagens as a function of pH in solution were measured as well and demonstrated in Figure 6. It was not hard to see that the similar variation tendencies for the zeta potentials of all the samples could be observed clearly. Significantly, the isoelectric point of virgin collagen was approximately at $\text{pH} = 4.9$, by contrast, the isoelectric points of PAM grafted collagens shifted to the higher

pH in turn with the weight feeding ratio of acrylamide increasing. Before the isoelectric points, they were significantly positively charged owing to protonation of $-\text{NH}_2$ groups, implying that presence of enough $-\text{NH}_2$ groups in the branched chains supported the flocculation of suspended kaolin particles with negative charges. It was worth noting that before $\text{pH} = 8.0$, the absolute values of zeta potential for grafted collagens were always higher than those of virgin collagen and increased gradually at the same pH condition as the feeding ratio of acrylamide increased. However, abnormal results were observed that the absolute values of zeta potential for grafted products became almost irregular after $\text{pH} 8.0$, which was possibly caused by the reason that the abundant $-\text{NH}_2$ groups were shielded by OH^- anions in alkaline solution, and the long PAM grafted chains were inclined to form curly random conformations freely, which would result in the ruleless alteration of the charge center.

Morphology

The microstructures of virgin collagen as well as PAM grafted collagen were observed directly by SEM, and the corresponding images were taken and given in Figure 7. As shown clearly in Figure 7 that the virgin collagen revealed their fairly regular and compacted structures with smooth surface, which implied their strong crystalline characteristic indirectly. However, drastic variation in morphology had taken place after grafting PAM chains onto the collagen backbone. Compared with the virgin collagen, there were much porous and looser surface structures in PAM grafted collagens, meanwhile, some tiny cracks were also found in these pores. Among these grafted samples, the CP12 exhibited the roughest surface laminar structure, which indicated that insertion of PAM moiety damaged the original structural regularity of collagen radically and contributed to the formation of porous structure eventually. This much more porous and rougher surfaces were expected to exert positive effect on the flocculation activity because of strong absorption caused by these plentiful pores.

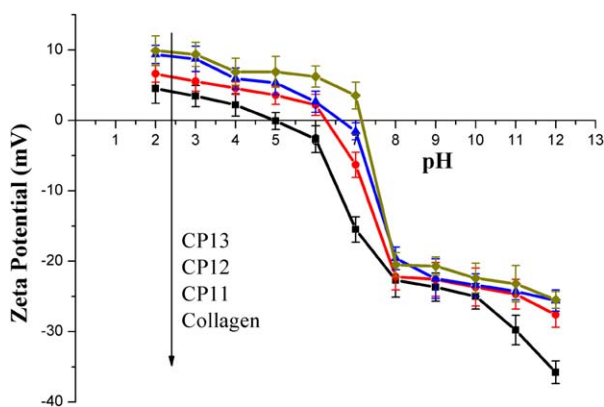


Figure 6. Zeta potential-pH profiles for collagen and various PAM grafted collagens. [Color figure can be viewed in the online issue, which is available at wileyonlinelibrary.com.]

Flocculation Property

The flocculation efficiencies of virgin collagen as well as grafted collagens in 3 g/L of kaolin suspension at pH = 4 were depicted in Figure 8. Obviously, virgin collagen, which was extracted from leather shavings, showed relevant ability for kaolin flocculation in itself due to the presence of a certain amount of $-NH_2$ groups in their molecular chains, which was very similar to chitosan.^{13,14,43} A common variation trend for all the investigated flocculants was clearly observed that the transmittances of supernatants increased quickly at the beginning and then reached a relative balance, and finally slowly decreased slightly

as the addition of flocculant gradually increased with the best dosage about 4–6 mg/L, which could be explained that insufficient flocculant was difficult to support complete settling for kaolin particles when the flocculant dosage was below 4 mg/L, on the contrary, flocculant-encapsulated kaolin particles would suspend more stably while the flocculant dosage was over 6 mg/L. In addition, CP12 performed the best and the maximal transmittance of supernatant could reach 85.88%, which indicated that the residual concentration of kaolin in supernatant suspension was significantly reduced to 13.8 mg/L, estimated in terms of the previously as-prepared calibration curve for kaolin suspension. In comparison with CP12 and CP13, CP11 performed poorly in kaolin flocculation, which was ascribed to its relatively lower grafting ratio. By contrast, the worst flocculating performance of virgin collagen was primarily caused by lower positively charge density and no chains with appropriate length to bring about enough bridging effect. These above mentioned results could be well established by the optical micrograph of the formed flocs.

The settling characteristics of 3 g/L of kaolin suspensions treated by collagen-based flocculants with their respective optimal dosages at pH 4 were also investigated, and variations of transmittance of the supernatant as a function of settling time were exhibited in Figure 9. For all the treated kaolin suspensions, a common tendency could be observed clearly that the transmittance of supernatant increased rapidly within 3.5 minutes and then persistently kept a small fluctuation around its maximum in the test scope. Obviously, virgin collagen had

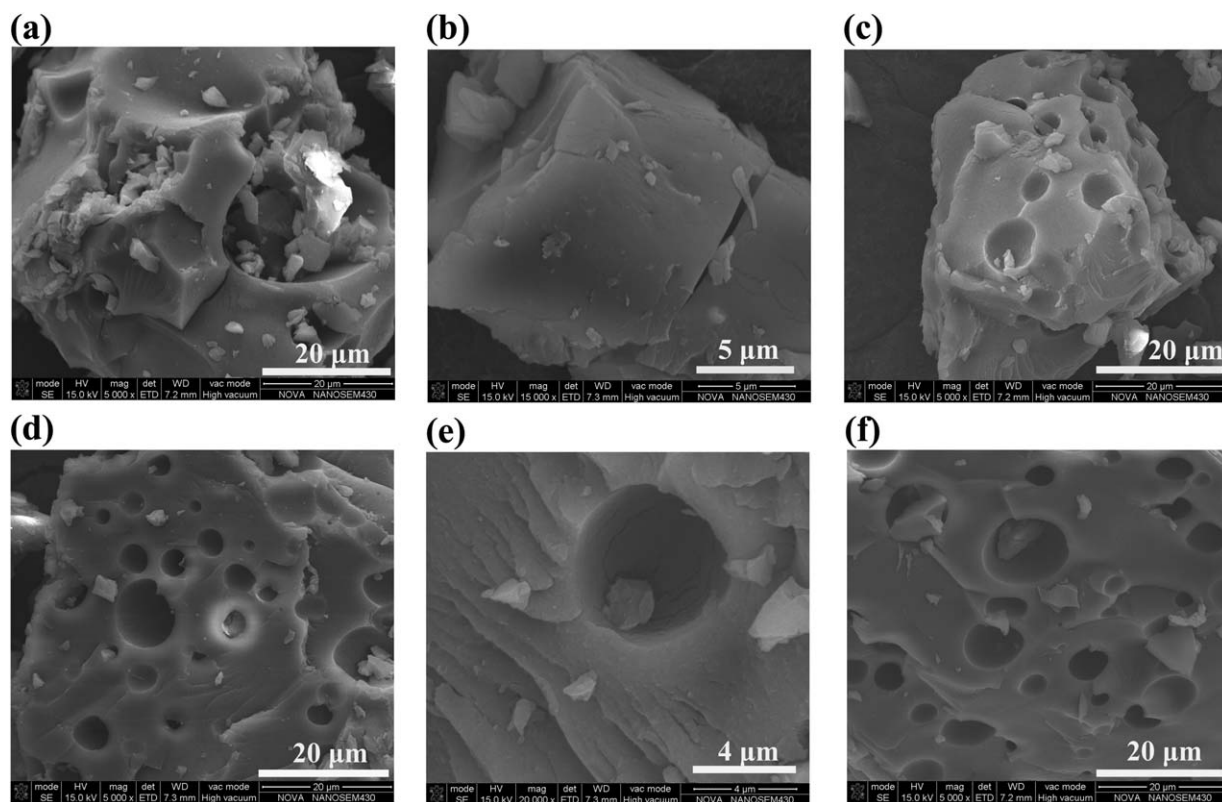


Figure 7. SEM micrographs of the various samples: (a) virgin collagen extracted from leather shavings; (b) surface of virgin collagen; (c) CP11; (d) CP12; (e) surface of CP12; (f) CP13.

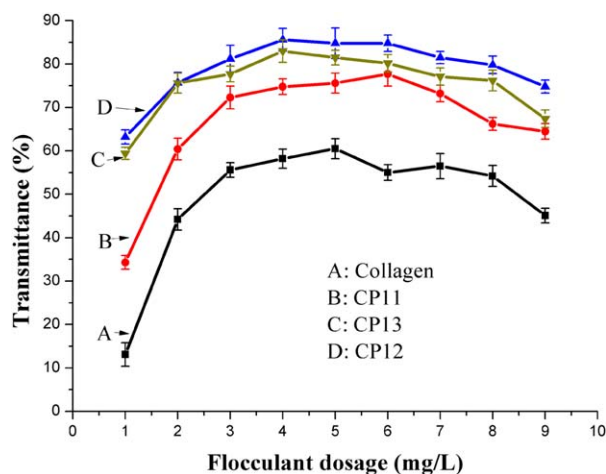


Figure 8. The flocculation efficiency of virgin collagen and various synthesized grades of PAM grafted collagen by stand jar test procedure. [Color figure can be viewed in the online issue, which is available at wileyonlinelibrary.com.]

the worst performance with the slowest flocculation rate about $15.9\% \cdot \text{min}^{-1}$, and the eventual transmittance of supernatant merely reached 65.5% approximately after complete flocculation, which indicated that virgin collagen could not be competent for kaolin flocculation, because the absence of sufficient positive charges and appropriate PAM branched chains resulted in difficulty inducing strong charges attraction and bridging effect. However, dramatic changes in flocculation ability had occurred after successfully grafting PAM branched chains onto collagen backbone. Compared with virgin collagen, all the modified products showed the better performances with the much quicker flocculation rate. Typically, CP12 performed

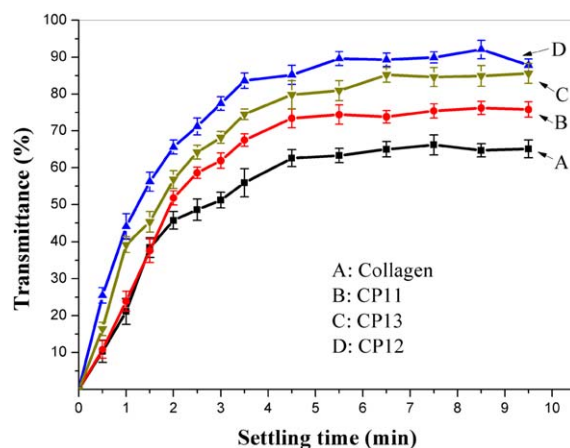


Figure 9. The extent of flocculation of 3 g/L kaolin suspensions with time by using virgin collagen and various PAM grafted collagens at respective optimal dosage. [Color figure can be viewed in the online issue, which is available at wileyonlinelibrary.com.]

the best with the fastest flocculation rate about $24\% \cdot \text{min}^{-1}$, which was 1.5 times than that of virgin collagen, and the final transmittance of supernatant could reach 92.1%. Similarly, CP13 and CP11 could also achieve the flocculation rate about 21.2 and $19.3\% \cdot \text{min}^{-1}$, respectively, moreover, their purification effects were obviously inferior to that of CP12, which was caused by their relatively lower grafting ratio.

Characterization of the Flocs and Flocculation Mechanism

The morphologies of the formed flocs obtained from kaolin suspensions with and without being treated by various collagen-based flocculants were exhibited in Figure 10. Obviously, the original kaolin particles were well dispersed and had hardly any

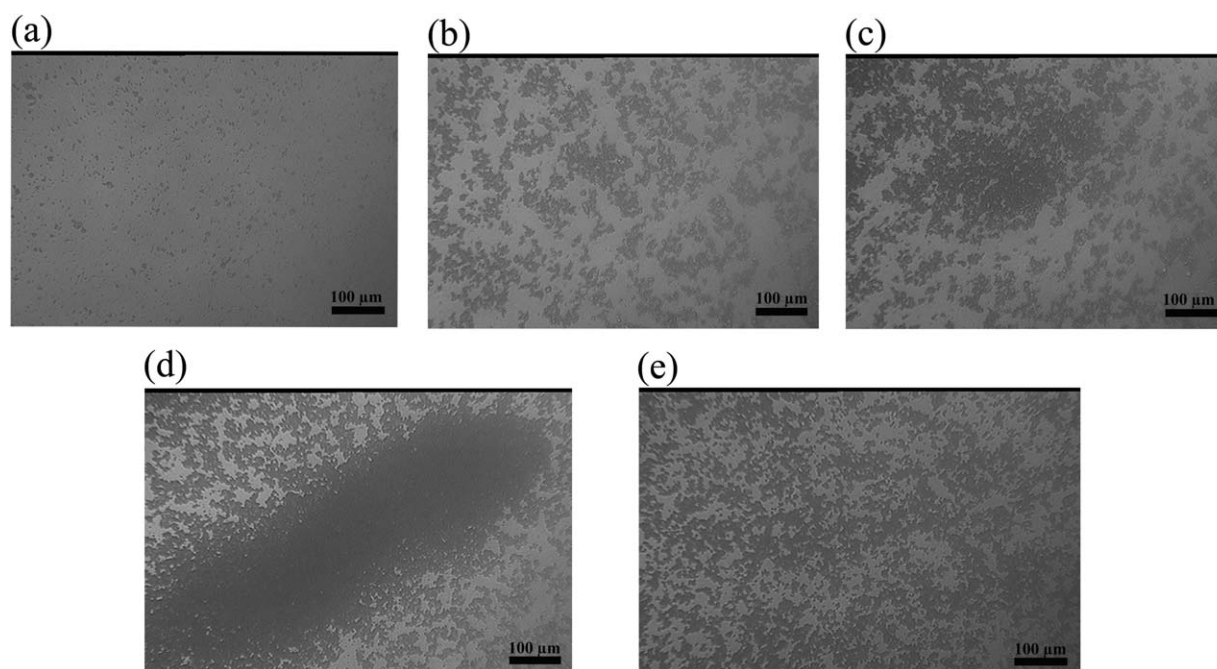


Figure 10. Images of kaolin particles (a) and the formed flocs obtained by treating kaolin suspensions with: (b) virgin collagen; (c) CP11; (d) CP12; (e) CP13.

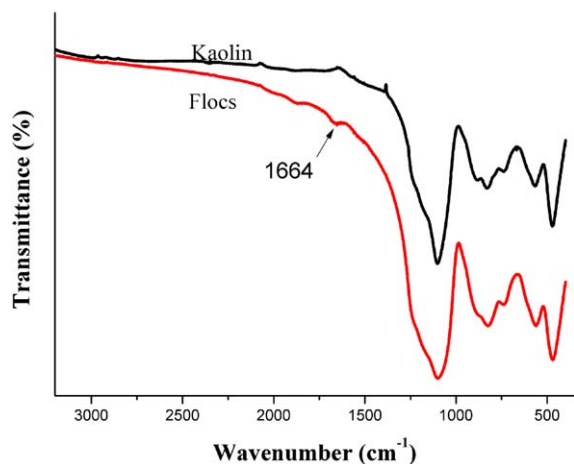


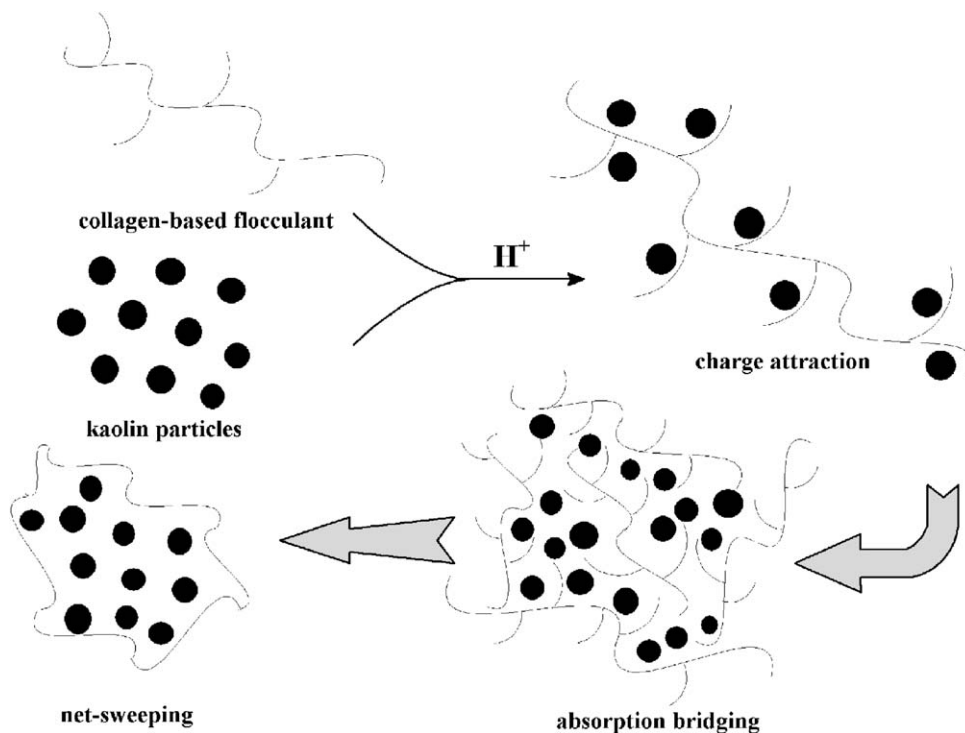
Figure 11. FTIR spectra of kaolin and the formed flocs obtained by treating kaolin suspension with collagen-based flocculant. [Color figure can be viewed in the online issue, which is available at wileyonlinelibrary.com.]

aggregation, which indicated that strong electrostatic repulsion could effectively inhibit the natural sedimentation of kaolin particles. By contrast, large and dense flocs were distinctly formed due to the addition of the collagen-based flocculants, and abundant kaolin particles got aggregated seriously and constituted various irregular and huge aggregates, which were closely joined together in dependence on the strong absorption bridging and net-sweeping effects, which were caused by the flocculants. The formation of extensive flocs not only contributed to accelerating sedimentation of kaolin particles, but also reflected the flocculating ability of the corresponding flocculant from

another perspective that the flocculant CP12 had the best flocculation performance.

The interactions between collagen-based flocculants and kaolin particles were also further studied to reveal the possible flocculation mechanism, and the FTIR spectra of the formed flocs and kaolin particles were also illustrated in Figure 11. As was shown clearly that in the spectrum of kaolin, the keen-edged band at 1093 cm^{-1} was assigned to the stretching vibration of silicon-oxygen bond (Si—O—Si), in addition, the other two bands at 887 and 842 cm^{-1} were attributed to asymmetric in-plane flexural vibration of $\text{Si}(\text{CH}_3)_3$ groups, while the weak band around 740 cm^{-1} could be assigned to symmetric in-plane flexural vibration of $\text{Si}(\text{CH}_3)_3$ groups, which indicated that the used kaolin had undergone surface treatment and been endowed with good water dispersion. However, there was an additional weak peak not available before present in the FTIR spectrum of the formed flocs, and this peak assigned to the carbonyl groups (C=O) had shifted from 1656 to 1664 cm^{-1} in comparison with collagen-based flocculants, which strongly supported the fact that electrostatic attraction between kaolin particles and collagen-based flocculants had taken place.

Based on the morphology features and FTIR analysis of the formed flocs obtained from processed kaolin suspension, the flocculation mechanism of PAM grafted collagen was proposed and described in Scheme 2. As previously reported,^{22,24} a $-\text{NH}_2$ group could be easily protonized by gaining a H^+ ion from acidic solution, and the newly formed positively charged group ($-\text{NH}_3^+$) would be absorbed on the surface of negatively charged kaolin particles in accordance with electrostatic attraction. And PAM grafted collagen obviously supplied the



Scheme 2. Flocculation mechanism for collagen-based flocculant induced kaolin settling.

capability required for the protonation of abundant $-\text{NH}_2$ groups. Apparently, the flocculation abilities of PAM grafted collagen, in addition to strong charge attraction, were significantly improved by the bridging effect due to the introduction of long PAM branched chains. The huge surface area of kaolin particles gave countless bonding sites for protonized $-\text{NH}_2$ groups from different molecular chains, meanwhile, a collagen-based flocculant molecule with long PAM branched chains also could absorb many kaolin particles. Consequently, lots of kaolin particles were trapped together. Moreover, much more residual free kaolin particles could be also easily netted by the formed aggregates. Ultimately, the constantly growing large and dense flocs would settle quickly. These multiple flocculation modes proceeded simultaneously and would not stop until the complete depletion of free collagen-based flocculants.

CONCLUSIONS

In summary, we demonstrated a facile, cost-effective, and conventional method to prepare an efficient flocculant for kaolin flocculation by grafting PAM chains onto the collagen, which was directly extracted from leather shavings via alkali hydrolysis. A series of experimental results adequately indicated that the PAM chains had been successfully inserted onto the collagen backbone, and the grafting ratios of CP11, CP12, and CP13 were 67.3, 82.1, and 70.4%, respectively. In addition, TGA results also implied that the length of PAM branched chains got shorter gradually as the feeding proportion of acrylamide monomers increased. Morphological analysis and structural analysis of the PAM grafted collagen showed that the modified collagen possessed much more porous and rougher surface structures and were also deprived of strong crystalline performance when compared with virgin collagen. Moreover, improvement in the positively charge density of modified collagen were also observed, which was induced by the easy protonation of abundant $-\text{NH}_2$ groups in the PAM branched chains. Furthermore, the results obtained from jar test showed that the CP12 performed best in kaolin flocculation, accompanying with the production of abundant large and dense flocs for rapid settlement. Meanwhile, a suitable flocculation mechanism was also proposed to explain its flocculation process based on analyzing the formed flocs. More significantly, this article has also provided a brand-new perspective to solve the both worrisome problems for years that ecological threat derived from chromed leather wastes and wastewater generated by mining industry has become increasingly more serious.

ACKNOWLEDGMENTS

The authors are sincerely grateful for the financial support from the National Natural Science Foundations of China (No. 21075043) and the Fundamental Research Funds for the Central Universities (No. 2011ZM0008).

REFERENCES

1. Maha Lakshmi, P.; Sivashanmugam, P. *Sep. Purif. Technol.* **2013**, *116*, 378.
2. Alvarez, M. S.; Moscoso, F.; Rodriguez, A.; Sanroman, M. A.; Deive, F. *J. Bioresour. Technol.* **2013**, *146*, 689.
3. Santos, I. D.; Dezotti, M.; Dutra, A. J. B. *Chem. Eng. J.* **2013**, *226*, 293.
4. Saranya, R.; Arthanareeswaran, G.; Dionysiou, D. D. *Chem. Eng. J.* **2014**, *236*, 369.
5. Rahul, R.; Jha, U.; Sen, G.; Mishra, S. *Int. J. Biol. Macromol.* **2014**, *63*, 1.
6. Yang, Z.; Yan, H.; Yang, H.; Li, H.; Li, A.; Cheng, R. *Water Res.* **2013**, *47*, 3037.
7. Feng, J.-J.; Zhang, P.-P.; Wang, A.-J.; Liao, Q.-C.; Xi, J.-L.; Chen, J.-R. *New J. Chem.* **2012**, *36*, 148.
8. Chen, D.; Chen, Q.; Ge, L.; Yin, L.; Fan, B.; Wang, H.; Lu, H.; Xu, H.; Zhang, R.; Shao, G. *Appl. Surf. Sci.* **2013**, *284*, 921.
9. Khanna, A.; Shetty, K. V. *Environ. Sci. Pollut. Res. Int.* **2013**, *20*, 5692.
10. Ghaedi, M.; Pakniat, M.; Mahmoudi, Z.; Hajati, S.; Sahraei, R.; Daneshfar, A. *Spectrochim Acta Part A* **2014**, *123*, 402.
11. Kadirova, Z. C.; Katsumata, K.-i.; Isobe, T.; Matsushita, N.; Nakajima, A.; Okada, K. *Appl. Surf. Sci.* **2013**, *284*, 72.
12. Helena, P.; Miia, H.; Sirkka, L. M. *J. Appl. Polym. Sci.* **2014**, *131*, 40448.
13. Yadav, M.; Sand, A.; Behari, K. *Int. J. Biol. Macromol.* **2012**, *50*, 1306.
14. Li, J.; Song, X.; Pan, J.; Zhong, L.; Jiao, S.; Ma, Q. *Int. J. Biol. Macromol.* **2013**, *62*, 4.
15. Ali, S. A.; Pal, S.; Singh, R. P. *J. Appl. Polym. Sci.* **2010**, *118*, 2592.
16. Pourjavadi, A.; Fakoorpoor, S. M.; Hosseini, S. H. *Carbohydr. Polym.* **2013**, *93*, 506.
17. Singh, R. P.; Pal, S.; Rana, V. K.; Ghorai, S. *Carbohydr. Polym.* **2013**, *91*, 294.
18. Lin, Q.; Qian, S.; Li, C.; Pan, H.; Wu, Z.; Liu, G. *Carbohydr. Polym.* **2012**, *90*, 275.
19. Rani, P.; Mishra, S.; Sen, G. *Carbohydr. Polym.* **2013**, *91*, 686.
20. Mishra, S.; Sen, G. *Int. J. Biol. Macromol.* **2011**, *48*, 688.
21. Nasim, T.; Panda, A. B.; Bandyopadhyay, A. *Int. J. Biol. Macromol.* **2013**, *58*, 140.
22. Yang, Z.; Yang, H.; Jiang, Z.; Cai, T.; Li, H.; Li, H.; Li, A.; Cheng, R. *J. Hazard. Mater.* **2013**, *254-255*, 36.
23. Jiang, X.; Qi, Y.; Wang, S.; Tian, X. *J. Hazard. Mater.* **2010**, *173*, 298.
24. Jiang, X.; Cai, K.; Zhang, J.; Shen, Y.; Wang, S.; Tian, X. *J. Hazard. Mater.* **2011**, *185*, 1482.
25. Fang, R.; Cheng, X.; Xu, X. *Bioresour. Technol.* **2010**, *101*, 7323.
26. Wang, J. P.; Yuan, S. J.; Wang, Y.; Yu, H. Q. *Water Res.* **2013**, *47*, 2643.
27. Sirviö, J.; Honka, A.; Liimatainen, H.; Niinimäki, J.; Hormi, O. *Carbohydr. Polym.* **2011**, *86*, 266.
28. Ocak, B. *J. Environ. Manage* **2012**, *100*, 22.
29. Paul, R.; Adzet, J. M.; Brouta-Agnés, M.; Balsells, S.; Esteve, H. *Dyes Pigments* **2012**, *94*, 475.

30. Malaisamy, R.; Lepak, L.; Spencer, M.; Jones, K. L. *Sep. Purif. Technol.* **2013**, *115*, 114.
31. Choy, A. T.; Leong, K. W.; Chan, B. P. *Acta Biomater.* **2013**, *9*, 4661.
32. Wang, J. P.; Chen, Y. Z.; Yuan, S. J.; Sheng, G. P.; Yu, H. Q. *Water Res.* **2009**, *43*, 5267.
33. Erdem, M.; Ozverdi, A. *J. Hazard. Mater.* **2008**, *156*, 51.
34. Swarnalatha, S.; Ganesh Kumar, A.; Tandaiyah, S.; Sekaran, G. *J. Chem. Technol. Biotechnol.* **2009**, *84*, 751.
35. Oliveira, L. C. A.; Guerreiro, M. C.; Gonçalves, M.; Oliveira, D. Q. L.; Costa, L. C. M. *Mater. Lett.* **2008**, *62*, 3710.
36. Wionczyk, B.; Apostoluk, W.; Charewicz, W. A.; Adamski, Z. *Sep. Purif. Technol.* **2011**, *81*, 237.
37. Kantarli, I. C.; Yanik, J. *J. Hazard. Mater.* **2010**, *179*, 348.
38. Yang, Q.; Qin, S.; Chen, J.; Ni, W.; Xu, Q. *J. Appl. Polym. Sci.* **2009**, *113*, 4015.
39. Liu, H.; Yang, X.; Zhang, Y.; Zhu, H.; Yao, J. *Water Res.* **2014**, *59*, 165.
40. Yang, Z.; Li, H.; Yan, H.; Wu, H.; Yang, H.; Wu, Q.; Li, H.; Li, A.; Cheng, R. *J. Hazard. Mater.* **2014**, *276*, 480.
41. Yang, Z.; Degorce-Dumas, J. R.; Yang, H.; Guibal, E.; Li, A.; Cheng, R. *Environ. Sci. Technol.* **2014**, *48*, 6867.
42. Yang, Z.; Wu, H.; Yuan, B.; Huang, M.; Yang, H.; Li, A.; Bai, J.; Cheng, R. *Chem. Eng. J.* **2014**, *244*, 209.
43. Zhu, H.; Sun, H.; Wang, F.; Zou, J.; Fan, J. *J. Appl. Polym. Sci.* **2012**, *125*, 2646.